IEEE Transactions on Nuclear Science, Vol. NS-32, No. 5, October 1985

THERMAL AND STRUCTURAL ANALYSIS OF RING COMPONENTS BY THE FINITE ELEMENT METHOD *

Rodulfo Alforque, and Sushil Sharma
National Synchrotron Light Source
Brookhaven National Laboratory
Upton, New York 11973

INTRODUCTION

In a previous report[1], a thermal study was made in order to determine the effects of a shift in the electron vertical orbital plane, and the resulting displacement of the wiggler photon beam striking the inner surface of the vacuum chamber. Since then, due to some changes in the physical parameters of the vacuum chamber, a new design had been developed. The new geometry is quite different from the one described in [1], due primarily to an increase in the chamber vertical aperture which was opened to 23 mm. from an initial opening of 6 mm.

Subsequently, a new study was conducted for this new chamber design that included a structural analysis in order to determine the stresses and deflections of the vacuum chamber due to the combined thermal and mechanical loading. It should be noted that various geometrical models were analyzed before the final geometry was decided. This report will only describe in detail the results of the thermal and structural analysis of the final geometry using the finite element code, ANSYS[3].

FINITE ELEMENT MODEL

The region of interest in the vacuum chamber was developed into a 2-dimensional finite element mesh. A fine mesh was used in the region where the gaussian-distributed heat load was applied in order to achieve a more accurate approximation. The full finite element model consisted of a total of 397 elements.

The chamber is made of silicon-magnesium aluminum alloy similar to 6063-T5 but stress relieved to a yield strength of 23 ksi. The areas of particular interest in this chamber were the inner surface exposed to the photon beam, and the cooling channel wall. The inner surface should not reach temperatures beyond the corresponding yield point of the material and the cooling channel wall temperatures should not be at levels that could initiate nucleate boiling caused by localized heating.

The element type that was used in the thermal model was a 2-D isoparametric thermal solid. The thermal run would produce the temperature distribution over the whole model. This distribution is then passed to the structural model for the subsequent stress and deflections analysis; The thermal element, Stif55, was converted into a 2-D isoparametric solid structural element, Stif42, for the structural portion of the analysis.

The actual geometry of the vacuum chamber is so complex that it is very difficult to predict accurately the actual stresses. Two structural models have been used, however, in order to bracket the possible state of stress during machine operation. The two analytical models are:

a) Plane Stress Model

This model gives the lower bound of the state of stress of the vacuum chamber. This assumes no restraint in the z-direction thereby allowing full extension in that direction with no resulting stresses; The prevailing load is the pressure load.

b) Plane Strain Model

The stresses from this model represent the worst possible state of stress that can occur in the chamber. The z-direction strain is zero, implying a rigid restraint in that direction thus causing a high stress, S_z, primarily due to the thermal load.

LOADS AND BOUNDARY CONDITIONS

At full power, *i.e.* E = 2.5 Gev, & I = 500 ma, and with a vertical displacement y mm., the power density, $P(y)$, at source distance, D = 10 m., can be expressed as [see ref. 2]:

$$P(y) = 88.72F(\gamma\varphi) \tag{1}$$

where,

$$F(\gamma\varphi) = 0.4375e^{-\frac{1}{2}\left(\frac{0.49y}{0.608}\right)^2} \tag{1a}$$

The maximum power density on the vacuum chamber surface occurs at an angle of 9.16° to the surface and at a distance, D = 6.49 m., from the source [1]. The beam power density striking the chamber at this distance is:

$$P_1(y) = \left(\frac{10}{6.49}\right)^2 P(y) \tag{2}$$

Integrating eq. (2) over the vertical spectrum gives the heat carried by the photon beam. The component of this heat absorbed by the vacuum chamber is :

$$P_T = 2\int_0^\infty P_1(y) sin 9.16^o dy \tag{3}$$

* Work performed under the auspices of the U.S. Department of Energy.

0018-9499/85/1000-3051$01.00© 1985 IEEE

If the chamber intercepts the full vertical width of the beam at full power ($I = 500ma$), the power absorbed by the thermal model is 30 watts per mm. of chamber length. This power was distributed to 13 nodal points in an appproximately gaussian distribution, and six load cases were studied; The 6th load case simulated partial but most of the beam striking the vacuum chamber.

In addition, load cases 5 and 6 were run with varying beam current from 100 to 500 ma. In all cases, heat removal was achieved by applying a convective boundary condition along the wall of the cooling channel.

Fig.1 shows some relevant parameters regarding the loads and boundary conditions. The structural model was given symmetry boundary condition at appropriate areas. A pressure load of 14.7 psi was applied along all surfaces exposed to the atmosphere and an average water pressure of 70 psi was applied to the elements along the wetted perimeter of the cooling channel.

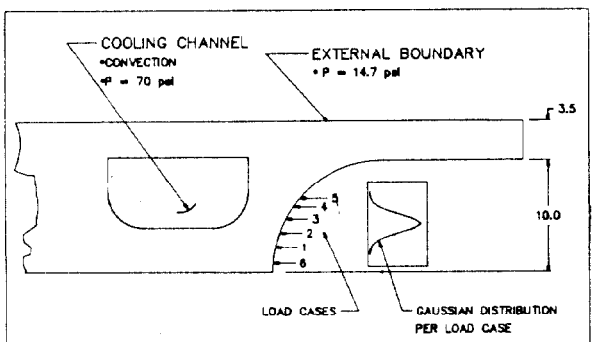

Fig. 1: LOADS & BOUNDARY CONDITIONS

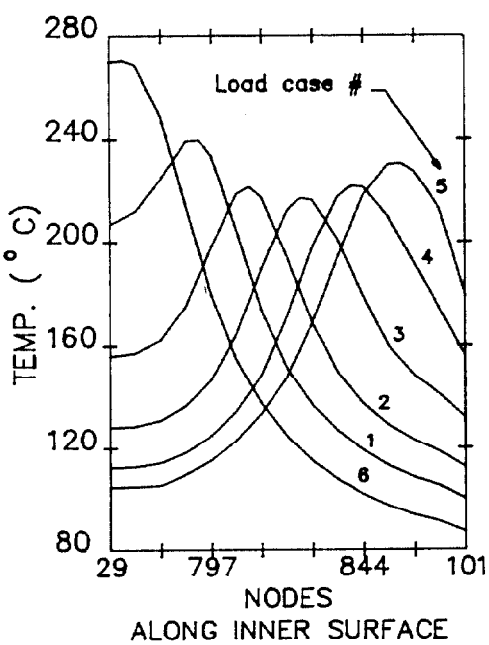

Fig.2: SURFACE TEMPERATURES

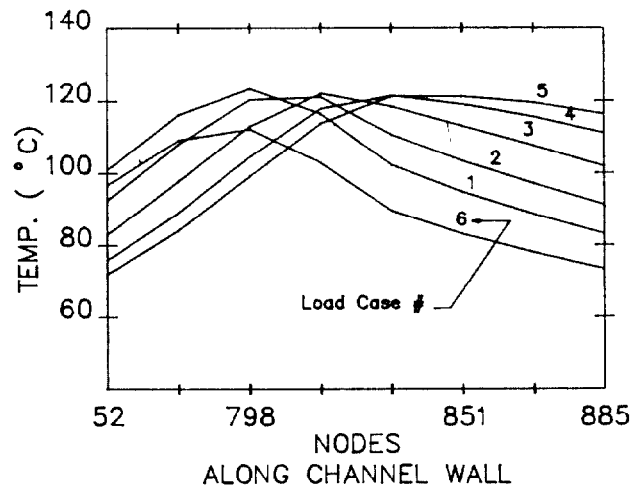

Fig.3: CHANNEL WALL TEMP.

RESULTS

a) Thermal Model

The results of a steady state solution of the thermal model at full power for the six load cases are shown in Figs.2,& 3. The inner surface of the vacuum chamber would reach a maximum of $270°C$ which is the peak temperature for load case 6. This temperature is well below the melting point of aluminum which is $615°C$.

At full power, the cooling channel wall will attain a maximum of $123°C$.This corresponds to about 30 psia saturation pressure for water, hence if the cooling water is maintained well above 30 psia no nucleate boiling could begin.The total pressure drop required along the cooling channel is about 20 psi, and since the available supply pressure of the cooling water is 90 psi, there is ample factor of safety to avoid boiling within the channel even at full power.

b) Plane Stress Model

The maximum deflection along the y-axis is about 0.175 mm. and this occurs, as expected, along A-A in Fig. 1. There is very little variation in the stresses and deflections for the six load cases, since obviously, the dominant structural loading is the pressure load. The maximum stress intensity, which is about $4.7ksi$ for load case 6 is not of critical concern since the temperatures there are low enough that the material strength are still very nearly room temperature values. However, in load case 5, the region where the highest temperature occurs deserves some examination. This temperature is $231°C$ and the corresponding yield strength of the material at this temperature is about $5ksi$. The stress intensity at this node is about $2.7ksi$. Obviously, the factor of safety in this situation is only roughly 2. Fig. 4 is a typical stress contour plot.

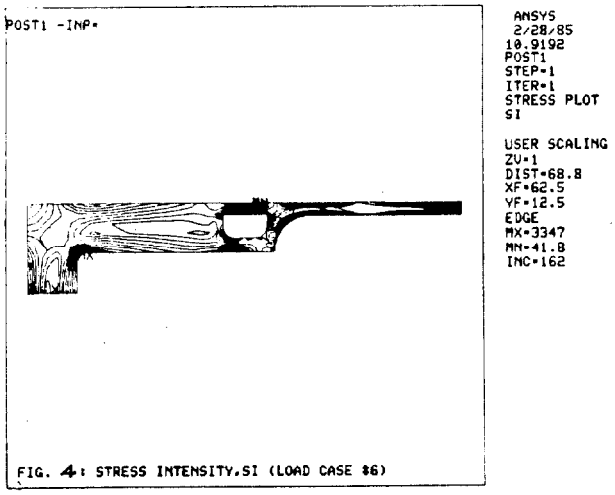

FIG. 4: STRESS INTENSITY.SI (LOAD CASE #6)

c) Plane Strain Model

Although the deflections (U_y) are essentially the same as in (b), the stresses are quite high when the plane strain boundary condition is imposed. These deflections, however, do not include the effects of the bending moments due to the chamber supports. Therefore, we decided to run the analysis at increasing beam currents starting from I = 100 ma at the same beam energy. For each run, the thermal parameters , such as the bulk water temperature and the film coefficient, were modified to reflect the corresponding heat loading. Fig. 5 summarizes the temperatures and stress intensities along the inner surface of the chamber. Indeed, as the beam current goes beyond 200 ma the stress levels will exceed the corresponding yield point. Beyond the yield point, however, the corresponding stress intensities are no longer realistic since the solution presented here is based on a linear, elastic formulation.

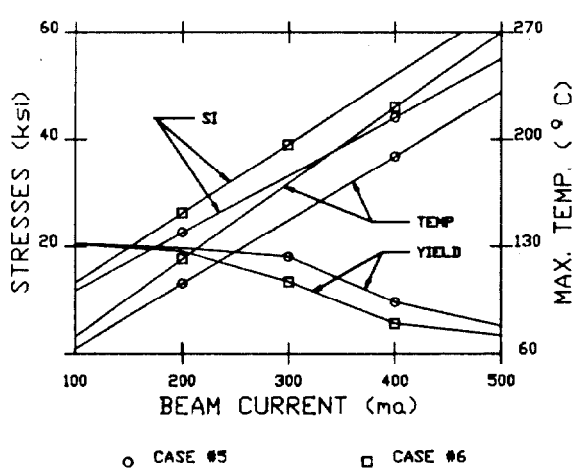

Fig.5: PLANE STRAIN MODEL

CONCLUSIONS

In view of the above results, when the plane stress boundary conditions are applicable, the vacuum chamber design looks acceptable even at full power. On the other hand, when there is absolute fixity in the z-direction, *i.e.*, the plane strain boundary condition exists, operation above 200 ma seems seriously questionable. It is obvious that material yielding will occur at higher currents, and permanent material set can happen that may compromise the structural integrity of the affected areas. We have mentioned at the outset that the actual condition can be bracketed by the plane-stress/plane-strain models; Unfortunately, however, due to various restraints along the length of the chamber, the real case is closer to a plane strain situation. Since this analysis is based on a linear, elastic formulation and the stresses are greater than the yield point at higher currents, it might be useful to look at the situation more closely using the non-linear approach.

In closing, we would like to mention that a numerical study was also done on the water-cooled beam stop that sits inside the vacuum chamber. Fig. 6 shows the $3-D$ finite element mesh, but due to space limitation we are unable to present the results of such analysis in this paper.

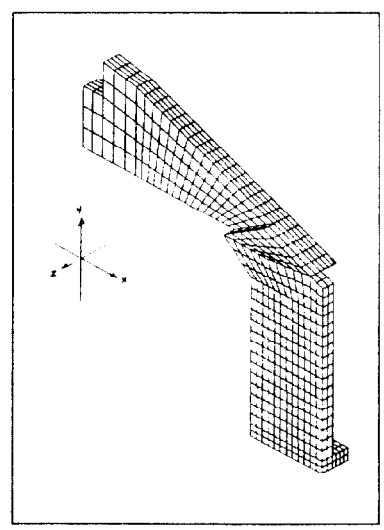

Fig.6: BEAM STOP: FEM Model

REFERENCES

1) *Vacuum Ring Exit Chamber Temperatures Due to Wiggler Beam Heating*, S. Sharma and S. Ulc, BNL-34314, January, 1984

2) *X-Ray Power Distribution From Multipole Wiggler Magnets*, W. Thomlinson, NSLS Internal Report, April 1983

3) *ANSYS, General Purpose Finite Element Code*, Swanson Analysis Systems Inc., Houston, PA 15342

ACKNOWLEDGEMENT

We are grateful to Hank Hsieh and Sam Krinsky for their helpful suggestions and discussions during the course of this work.